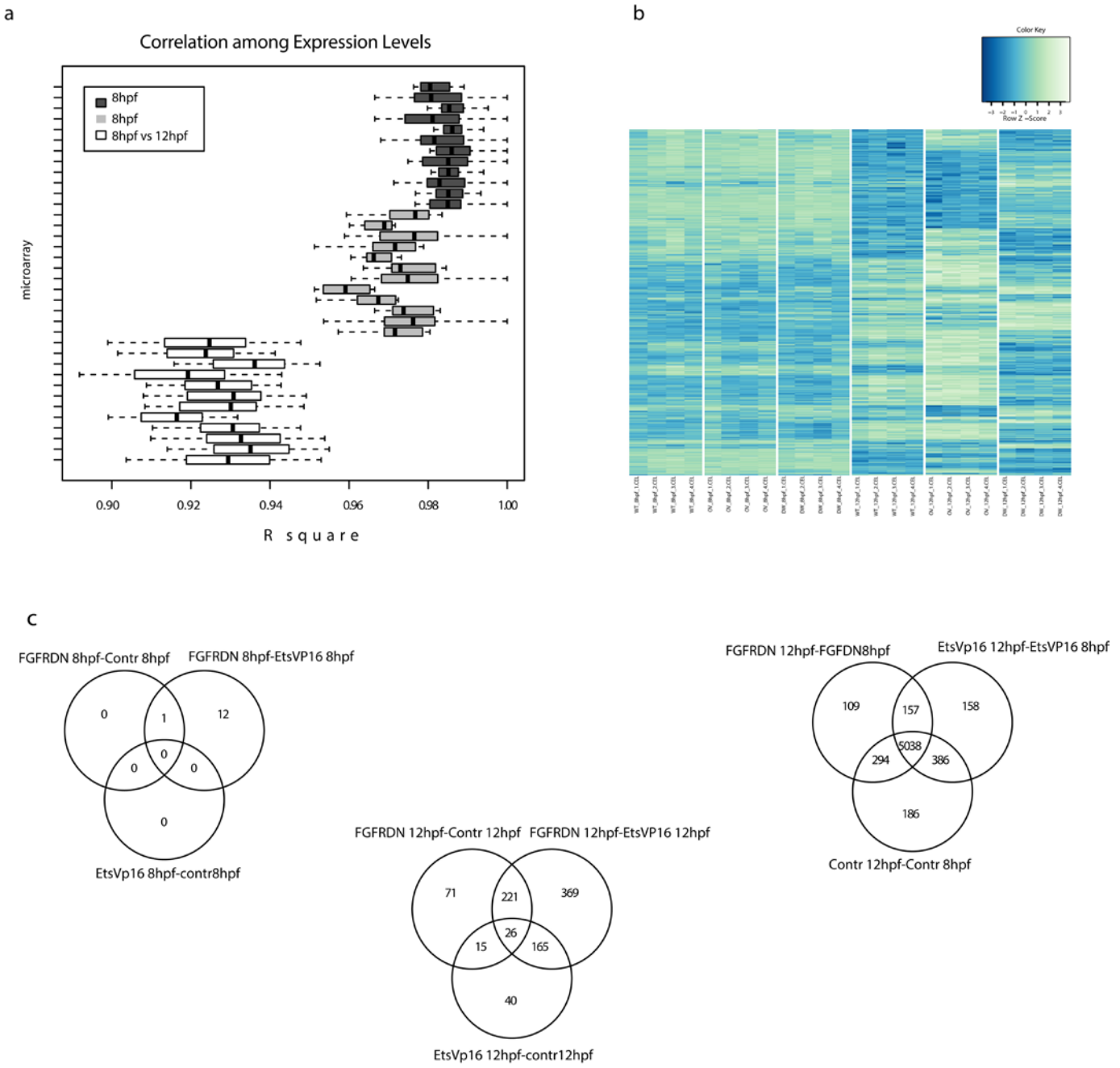

Supplementary Fig. 1 **Quality analysis of whole expression dataset:** a) Correlation analysis among samples using normalized expression levels from the whole microarrays. Boxplots show the distribution of the R^2 values for each sample compared to all the others at 8 hpf (dark gray), 12 hpf (light gray) and 8 *vs* 12 hpf. b) Heatmap showing the expression levels among the different samples for all the probesets resulting significantly differentially expressed in at least one comparison. c) Venn diagrams illustrating the numbers of significantly differentially expressed transcripts for each comparison split in three groups: comparisons at 8 hpf, comparisons at 12 hpf and comparisons at 8 *vs* 12 hpf.

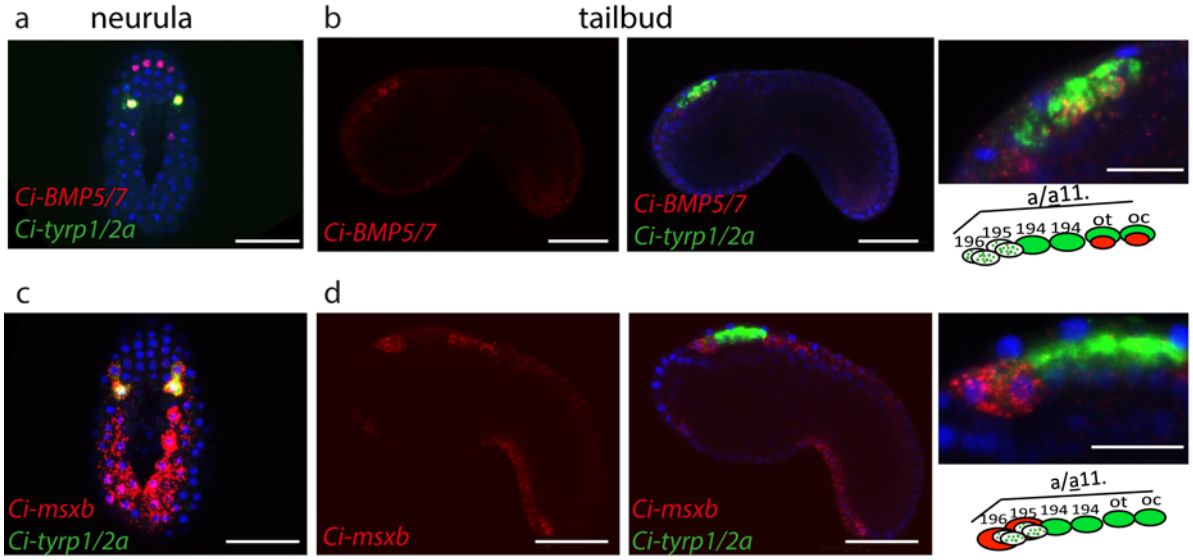

Supplementary Fig. 2 **Expression pattern of *Ci-BMP5/7* and *Ci-Msxb***: (a-b) Double Fluorescent WMISH of *Ci-BMP5/7* and *Ci-Msxb* (red) with *Ci-tyrp1/2a* (green). (a) expression of *Ci-BMP5/7* at neurula stage is confined to the anterior border of the neural plate and in the a10.97 cell pair as confirmed by *Ci-tyrp1/2a* localization. (b) Lateral view of middle tailbud stage, *Ci-BMP5/7* is weakly expressed in the anterior CNS and in the otolith and ocellus melanocyte precursors (a11.193s). (c) at neurula stage expression of *Ci-msxb* is detected along the lateral border of the neural plate including PCPs (a10.97s and a10.98s, as confirmed by *Ci-tyrp1/2a*; (d) at middle tailbud stage, *Ci-msxb* become excluded from a11.193s/a11.194s as confirmed by *Ci-tyrp1/2a* detection but it conserves the expression in a11.95s/a11.196s that present a very faint expression of *Ci-tyrp1/2a*. Zoom and schematic representation of cells expressing *Ci-tyrp1/2a* and *Ci-BMP5/7* and *Ci-msxb*, respectively, adapted from Cole and Meinertzhagen, 2004; (a,c) vegetal view, anterior is up; (b,d) lateral view, anterior is to the left. Scale bar 50 µm. nuclear staining by DAPI (blue).

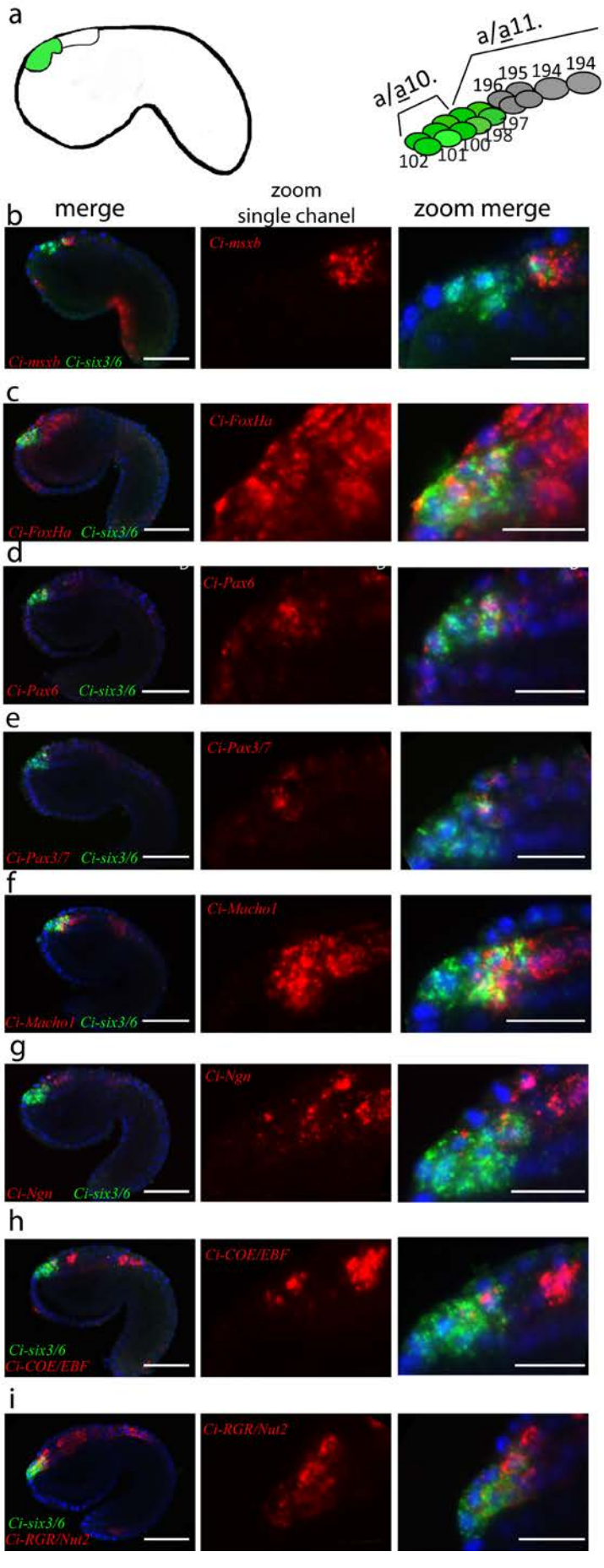
a
a/a11.
a/a10.
196
195
194
194
197
198
100
101
102
b
merge
zoom
single chanel
zoom merge
Ci-msxb
Ci-msxb Ci-six3/6
c
Ci-FoxHa
Ci-FoxHa Ci-six3/6
d
Ci-Pax6
Ci-Pax6 Ci-six3/6
e
Ci-Pax3/7
Ci-Pax3/7 Ci-six3/6
f
Ci-Macho1
Ci-Macho1 Ci-six3/6
g
Ci-Ngn
Ci-Ngn Ci-six3/6
h
Ci-COE/EBF
Ci-six3/6
Ci-COE/EBF
i
Ci-RGR/Nut2
Ci-six3/6
Ci-RGR/Nut2

Supplementary Fig.3 **Co-localization of *Ci-Six3/6* with anterior CNS markers**: (a) Schematic illustration of CNS *Ciona* tailbud stage (left) with part of a9.50 and a9.49 derived cells (right) showing Six3/6 expression domain (green), adapted from Cole and Meinertzhagen, 2004. (b-i) Double WMISH for TFs Up-regulated when comparing $FGFR^{DN}$ *vs* Control: *Ci-msxb* (b), *Ci-FoxHa* (c), *Ci-Pax6* (d), *Ci-Pax3/7* (e), *Ci-Macho1* (f), *Ci-Ngn* (g), *Ci-COE* (h), *Ci-RGR/Nut2* (i) expression domains (red) are compared to *Ci-Six3/6* expression (green), considered as a molecular marker for the anterior sensory vesicle. Lateral view, anterior is on the left. Scale bar 50µm; scale bar 20µm for zoomed embryos; nuclear staining by DAPI (blue).

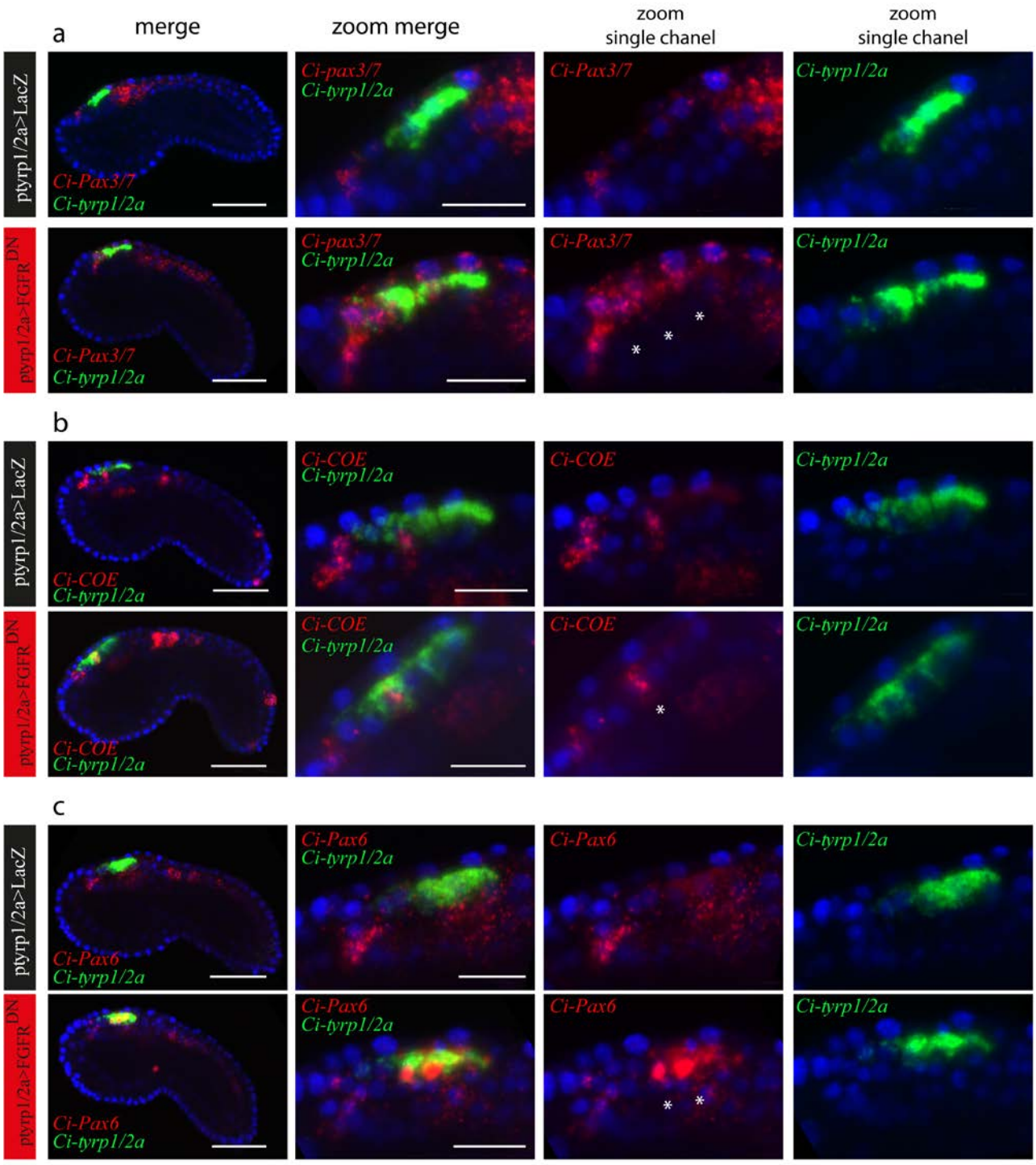

Supplementary Fig.4 **FGF signaling inhibits anterior CNS markers in the adjacent PCPs:** Double Fluorescent WMISH of *Ci-Pax3/7*(a), *Ci-COE* (b) and *Ci-Pax6* (c)(red) with *Ci-tyrp1/2a* (green) on electroporated embryos with ptyrp1/2a>LacZ (black box) and ptyrp1/2a>FGFR^{DN} (red box). (a) Control embryos: *Ci-Pax3/7* is expressed in anterior dorsal neural cells but is mostly excluded from *Ci-tyrp1/2a*$^{+}$ cells. FGFR^{DN} embryos: *Ci-Pax3/7* overlaps with *Ci-tyrp1/2a* in a10.97 derivatives (white asterisks). (b) Control embryos: *Ci-COE* is expressed in several neural cells but is almost excluded from *Ci-tyrp1/2a*$^{+}$ cells. FGFR^{DN} embryos: *Ci-COE* expression is clearly increased in *Ci-tyrp1/2a* expressing cells, in particular with a11.194s (white asterisks). (c) Control

embryos: *Ci-Pax6* is expressed all along the dorsal neural tube with a faint expression in *Ci-tyrp1/2a*$^{+}$ cells. FGFR^{DN} embryos: *Ci-Pax6* expression is strongly enhanced in *Ci-tyrp1/2a* expressing cells (white asterisks).

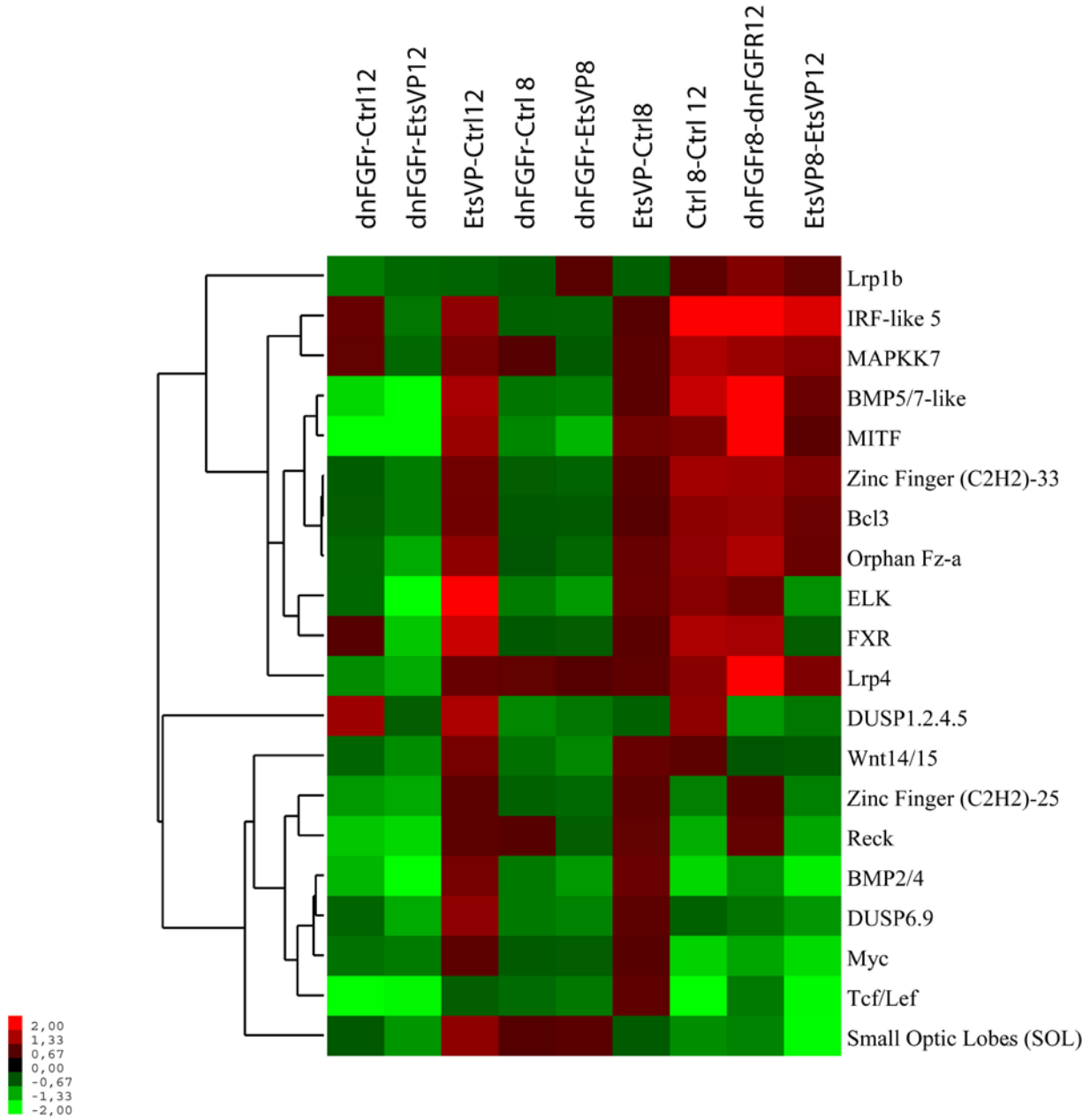

Supplementary Fig.5 **Hierarchical clustering and heat map for regulatory genes involved PCP fate specification**: expression values ($\log_2$ FC) consisting of 20 regulatory genes including, novel candidate regulators of PCP formation, FGF, BMP and Wnt signalling components; clustering was performed taking in account all three conditions (control, $FGFR^{DN}$, Ets:Vp16) at the two developmental stages (8 and 12 hpf); expression levels are colour coded with shades of red, green and black corresponding to an increase, decrease and no change in gene expression, respectively, as represented by the colour range below.

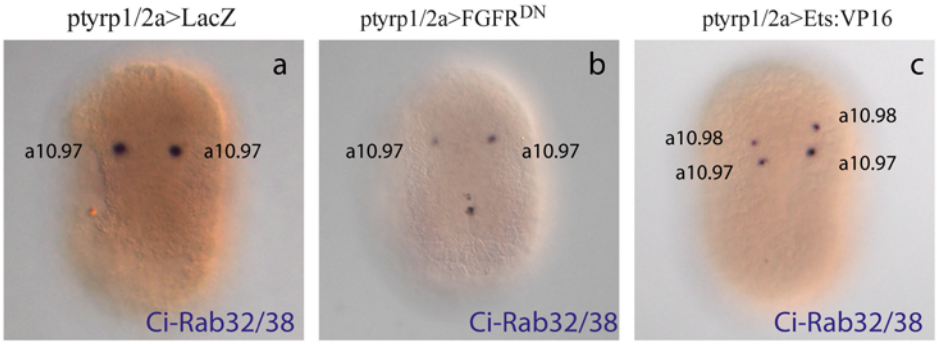

Supplementary Fig.6 **Differential expression of *Ci-Rab32/38* in FGF signaling pertubated embryos:** WMISH experiments using C*i-Rab32/38* antisense RNA as probe to reveal *Ci-Rab32/38* expression on electroporated embryos with ptyrp1/2a>LacZ (a), ptyrp1/2a>FGFR ^{DN} (b) and ptyrp1/2a>Ets:Vp16 (c) at neurul a stage (8hpf). *Ci-Rab32/38* is expressed in a10.97 cell pairs in control embryo (a); on FGF pertubated embryos its expression resulted reduced in a10.97 cell pairs when FGF signaling is blocked (b) while it appears expanded in a10.98 cells in ptyrp1/2a>Ets:VP16 embryos (c).

Supplementary Table-1: GO analysis on transcripts differential expressed when comparing FGFRDN to control at 8 and 12hpf

GO.id	n.uni	n.sel	p.uni	p.sel	p.value	adj.p	Definition
GO:0043473	43	13	0.204168843	1.431718062	3.78E-12	7.75E-09	pigmentation
GO:0009263	4	4	0.018992451	0.440528634	8.99E-09	0.0000184	deoxyribonucleotide biosynthetic process
GO:0006345	4	4	0.018992451	0.440528634	8.99E-09	0.0000184	loss of chromatin silencing
GO:0035059	4	4	0.018992451	0.440528634	8.99E-09	0.0000184	RCAF complex
GO:0030156	4	4	0.018992451	0.440528634	8.99E-09	0.0000184	benzodiazepine receptor binding
GO:0030050	5	4	0.023740563	0.440528634	8.06E-08	0.000164738	vesicle transport along actin filament
GO:0000074	239	28	1.134798917	3.083700441	0.000000176	0.000359713	regulation of cell cycle
GO:0004748	10	5	0.047481126	0.550660793	0.000000239	0.000488626	ribonucleoside-diphosphate reductase activity
GO:0030318	16	6	0.075969802	0.660792952	0.000000434	0.000885326	melanocyte differentiation
GO:0030178	104	16	0.493803713	1.762114537	0.000000627	0.001277442	negative regulation of Wnt receptor signaling pathway
GO:0042393	74	13	0.351360334	1.431718062	0.000000772	0.001574157	histone binding
GO:0051270	17	6	0.080717915	0.660792952	0.00000093	0.001894222	regulation of cellular component movement
GO:0005971	3	3	0.014244338	0.330396476	0.00000192	0.003918366	ribonucleoside-diphosphate reductase complex
GO:0048319	3	3	0.014244338	0.330396476	0.00000192	0.003918366	axial mesoderm morphogenesis
GO:0046022	3	3	0.014244338	0.330396476	0.00000192	0.003918366	positive reg. of transcription from RNA pol. II promoter during mitosis
GO:0048625	3	3	0.014244338	0.330396476	0.00000192	0.003918366	myoblast cell fate commitment
GO:0035182	3	3	0.014244338	0.330396476	0.00000192	0.003918366	female germline ring canal outer rim
GO:0030725	3	3	0.014244338	0.330396476	0.00000192	0.003918366	germline ring canal formation
GO:0007090	7	4	0.033236788	0.440528634	0.00000197	0.004008919	regulation of S phase of mitotic cell cycle
GO:0031489	7	4	0.033236788	0.440528634	0.00000197	0.004008919	myosin V binding
GO:0007052	79	13	0.375100897	1.431718062	0.0000025	0.005064511	mitotic spindle organization
GO:0043113	69	12	0.327619771	1.321585903	0.00000257	0.00521118	receptor clustering
GO:0007067	465	41	2.207872371	4.515418502	0.00000481	0.009743447	mitosis
GO:0051301	643	52	3.053036418	5.726872247	0.00000516	0.010448905	cell division
GO:0006260	405	37	1.922985613	4.074889868	0.00000539	0.010901444	DNA replication

GO:0007049	1130	80	5.365367267	8.810572687	0.0000059	0.011931903	cell cycle
GO:0042994	8	4	0.037984901	0.440528634	0.00000657	0.013286636	cytoplasmic sequestering of transcription factor
GO:0000916	8	4	0.037984901	0.440528634	0.00000657	0.013286636	contractile ring contraction involved in cell cycle cytokinesis
GO:0030538	8	4	0.037984901	0.440528634	0.00000657	0.013286636	embryonic genitalia morphogenesis
GO:0048619	8	4	0.037984901	0.440528634	0.00000657	0.013286636	embryonic hindgut morphogenesis
GO:0042475	95	14	0.451070699	1.54185022	0.00000716	0.014440386	odontogenesis of dentine-containing tooth
GO:0004866	64	11	0.303879208	1.211453744	0.00000853	0.017214596	endopeptidase inhibitor activity
GO:0007307	21	6	0.099710365	0.660792952	0.0000111	0.022398415	eggshell chorion gene amplification
GO:0000285	4	3	0.018992451	0.330396476	0.0000134	0.027079598	1-phosphatidylinositol-3-phosphate 5-kinase activity
GO:0021903	4	3	0.018992451	0.330396476	0.0000134	0.027079598	rostrocaudal neural tube patterning
GO:0007192	4	3	0.018992451	0.330396476	0.0000134	0.027079598	activation of adenylate cyclase activity by serotonin receptor signaling pathway
GO:0004771	4	3	0.018992451	0.330396476	0.0000134	0.027079598	sterol esterase activity
GO:0050580	4	3	0.018992451	0.330396476	0.0000134	0.027079598	2,5-didehydrogluconate reductase activity
GO:0007561	4	3	0.018992451	0.330396476	0.0000134	0.027079598	imaginal disc eversion
GO:0007500	9	4	0.042733014	0.440528634	0.0000182	0.036539142	mesodermal cell fate determination
GO:0031409	9	4	0.042733014	0.440528634	0.0000182	0.036539142	pigment binding
GO:0006726	9	4	0.042733014	0.440528634	0.0000182	0.036539142	eye pigment biosynthetic process
GO:0000799	15	5	0.071221689	0.550660793	0.0000183	0.036628797	nuclear condensin complex
GO:0004806	15	5	0.071221689	0.550660793	0.0000183	0.036628797	triglyceride lipase activity
GO:0004867	137	17	0.65049143	1.872246696	0.0000192	0.038379162	serine-type endopeptidase inhibitor activity

Supplementary Table-2: FGF hub genes in early PCPs					
Blast homology	**Ciona**	**Degree**	***p*value**	**Regulation**	**Fold Change**
NA	NA	778	0.001978	down	-1.122513
C3AR_MOUSE (O09047) C3a anaphylatoxin chemotactic receptor (C3a-R)	NA	776	0.001640	down	-2.0338864
YAJ8_SCHPO (Q09908) Hypothetical protein C30D11.08c in chromosome I	Ci-NF001	622	0.000758	up	1.4608647
RAB32_HUMAN (Q13637)Rab-32,RAB38_MOUSE (Q8QZZ8) Rab-38	Rab38,RAB32,ltd	590	0.002078	up	1.5973053
MAML3_HUMAN (Q96JK9) Mastermind-like protein 3	mam	474	0.002523	up	1.3477119
MAMC2_HUMAN (Q7Z304) MAM domain containing protein 2 precursor	NA	451	0.001639	down	-1.1346155
MYRIP_HUMAN (Q8NFW9) Rab effector MyRIP	MLPH	340	0.001672	up	2.8339636
FUCTC_DROME (P83088) Alpha-(1,3)-fucosyltransferase C (EC 2.4.1.-)	FucTA	169	0.000045	up	2.0985527